Published in final edited form as:
Ultrasound Med Biol. 2007 June ; 33(6): 950–958.

Molecular imaging with targeted perfluorocarbon nanoparticles: Quantification of the concentration dependence of contrast enhancement for binding to sparse cellular epitopes

Jon N. Marsh, **Kathryn C. Partlow**, **Dana R. Abendschein**, **Michael J. Scott**, **Gregory M. Lanza**, and **Samuel A. Wickline**
Center for Applied Nanomedicine, Departments of Internal Medicine, Biomedical Engineering, and Cellular Biology and Cell Physiology. Washington University, St. Louis, MO, USA

Abstract

Targeted, liquid perfluorocarbon nanoparticles are effective agents for acoustic contrast enhancement of abundant cellular epitopes (e.g. fibrin in thrombi) and for lower prevalence binding sites, such as integrins associated with tumor neovasculature. In this study we sought to delineate the quantitative relationship between the extent of contrast enhancement of targeted surfaces and the density (and concentration) of bound perfluorocarbon (PFC) nanoparticles. Two dramatically different substrates were utilized for targeting. In one set of experiments, the surfaces of smooth, flat, avidin-coated agar disks were exposed to biotinylated nanoparticles to yield a thin layer of targeted contrast. For the second set of measurements, we targeted PFC nanoparticles applied in thicker layers to cultured smooth muscle cells expressing the transmembrane glycoprotein “tissue factor” at the cell surface. An acoustic microscope was used to characterize reflectivity for all samples as a function of bound PFC (determined via gas chromatography). We utilized a formulation of *low-scattering* nanoparticles having oil-based cores to compete against *high-scattering* PFC nanoparticles for binding, to elucidate the dependence of contrast enhancement on PFC concentration. The relationship between reflectivity enhancement and bound PFC content varied in a curvilinear fashion, and exhibited an apparent asymptote (approximately 16 dB and 9 dB enhancement for agar and cell samples, respectively) at the maximum concentrations (~150 μg and ~1000 μg PFOB for agar and cell samples, respectively). Samples targeted with only oil-based nanoparticles exhibited mean backscatter values that were nearly identical to untreated samples (<1 dB difference), confirming the oil particles’ low-scattering behavior. The results of this study indicate that substantial contrast enhancement with liquid perfluorocarbon nanoparticles can be realized even in cases of partial surface coverage (as might be encountered when targeting sparsely populated epitopes), or when targeting surfaces with locally irregular topography. Furthermore, it may be possible to assess the quantity of bound cellular epitopes through acoustic means.

Keywords

molecular imaging; site-targeted contrast agent; nanoparticle; perfluorocarbon; tissue factor

Corresponding Author: Jon N. Marsh, C-TRAIN Group, Campus Box 8215, Cortex Building, Suite 101, 4320, Forest Park Avenue, St. Louis MO 63108, United States, Phone: 314-747-3045, Fax: 314-454-7490, Email: jnm@cvu.wustl.edu

INTRODUCTION

Ultrasound is a widely available clinical imaging modality and one of the most economical and flexible. However, its participation in the emerging discipline of molecular imaging has been featured less prominently in scientific literature than that of other imaging modalities until the recent advent of targetable ultrasound contrast agents (Liang et al. 2003). The first generation of specifically targeted acoustic contrast agents for ultrasound molecular imaging (reported in 1995) was liquid perfluorocarbon (PFC) nanoparticle emulsions (Lanza et al. 1995a;Lanza et al. 1995b;Wallace et al. 1995) and subsequently echogenic liposomes (Alkan-Onyuksel et al. 1996). Later studies with targeted microbubbles also have shown promise for sensitive molecular imaging (Klibanov et al. 1997;Villanueva et al. 1998;Lindner et al. 2000;Schumann et al. 2002;Leong-Poi et al. 2003), although their relatively large size (typically on the order of microns), susceptibility to destruction by insonant mechanical waves, and nonlinear response that renders quantification problematic stand as challenges to widespread adoption.

Although PFC nanoparticles are less sensitive contrast agents on a per particle basis, they may also be less liable to nonspecific signal enhancement events since larger concentrations (more binding events) are required to produce conspicuity. In certain cases (e.g., fibrin targeting in plasma thrombi), more than 20 dB of signal augmentation is achieved after binding to abundant molecular epitopes (Marsh et al. 2002a). The utility of these agents for contrast enhancement of other less abundant cellular epitopes (such as “tissue factor”) has been previously illustrated at higher frequencies (20+ MHz), using intravascular ultrasound for inflammation imaging in live animals (Lanza et al. 2000), and for isolated cell imaging with acoustic microscopy in vitro (Marsh et al. 2004). However, the relationship between the local abundance of molecular epitopes on cells and the local concentrations of nanoparticles that are required to impact backscatter from the targeted cell surfaces has not been quantified. The question is significant for clinical application because such data may provide insights into the lower limits of nanoparticle concentrations needed to create contrast after binding events, given the potential sparseness of molecular epitopes that might be available for targeting in certain pathologies. Additionally, knowledge of the specific nature of the dependence of enhancement on nanoparticle coverage could provide an avenue for estimation of the relative epitope density on a substrate from observed backscatter. This information might prove useful, for example, in quantifying the time-course of anti-angiogenic therapy for atherosclerosis through serial measurements of the vasa vasorum of atherosclerotic vessels with the application of nanoparticles targeted to $\alpha_v\beta_3$-integrin expression (Winter et al. 2006). Furthermore, such data could suggest a priori the appropriate candidates for detection with targeted nanoparticles (i.e. moderate or high epitope density and/or low targeting specificity) versus those that might better employ microbubbles for molecular imaging (low epitope density with high targeting specificity).

Accordingly, we targeted mixtures of standard “*high-contrast*” PFC nanoparticles and experimental “*low-contrast*” nanoparticles (made with oil-based cores, rather than PFC) to two types of samples in order to quantify the dependence of acoustic reflectivity on PFC concentration. The low-contrast oil-based nanoparticles were used to compete against the PFC agents for targeting sites on the substrate, so as to create selected levels of bound high-contrast nanoparticles at the surface. In one case, avidin-coated agar disks were exposed to biotinylated nanoparticle mixtures to target the sample surface. This artificial substrate was utilized in order to provide uniform, reproducible samples that ostensibly yielded the “simplest” targeting scenario, in which the nanoparticles were bound in a thin layer on a smooth and flat surface. The second sample group consisted of cultured smooth muscle cells that constitutively expressed tissue factor. Tissue factor, also known as thromboplastin or thrombokinase, is a transmembrane glycoprotein associated with the coagulation cascade. In normal vessels, tissue

factor is expressed at the plasma membrane of smooth muscle cells in the tunica media and fibroblasts in the adventitia (Moons et al. 2002). Tissue factor is normally not exposed to circulating blood unless the endothelial layer is damaged or an atheroma plaque ruptures, at which point tissue factor complexes with coagulation factor VII to initiate events leading to the generation of thrombin, and, ultimately, cross-linked fibrin strands that form the supporting network of a clot. Smooth muscle cells grown in culture and expressing tissue factor at the cell surface were targeted with nanoparticles using a specific polyclonal antibody (mAb) ligand against tissue factor. Although grown in controlled conditions on flat substrates, these samples provided a more complex and less uniform surface for targeting, due to the variability in configuration and shape of the cells, and in the level and distribution of tissue factor expression. In this case, nanoparticles could target the cells in vitro more densely and in a three-dimensional configuration, being able to bind along undulating cell surfaces, interstices, and pseudopods. For both agar and cellular samples, independent measurement of the total amount of bound PFC was possible through the use of gas chromatography, and enabled comparison with reflectivity enhancement on a sample-by-sample basis.

MATERIALS AND METHODS

Nanoparticle Formulation

The high contrast emulsions were formulated according to methods previously described (Lanza et al. 1996;Marsh et al. 2002a). The PFC emulsion was comprised of perfluoro-octyl bromide ("PFOB," 20% vol/vol, Exfluor Research Corporation, Round Rock, TX), a surfactant co-mixture (1.3%, wt/vol), and glycerin (1.7%, wt/vol). The surfactant co-mixture, which included a biotinylated phospholipid (1 mole % biotinyl cap dipalmatoyl-phosphotidylethanolamine, Avanti Polar Lipids, Inc., Alabaster, AL), was dissolved in chloroform, evaporated, dried in vacuum, and dispersed into water by sonication. The resulting suspension was blended with the PFOB and distilled, deionized water, and then emulsified for 30 to 60 seconds. The mixture was transferred to a microfluidizer (Microfluidics M-110S, Newton, MA) and continuously processed at 140 MPa for 4 minutes. The completed emulsion was placed in sealed vials and blanketed with nitrogen until use. Similar methods were used to formulate the low-contrast oil-based emulsion, by substitution of an equal volume percentage of safflower seed oil (Sigma-Aldrich, St. Louis, MO) in place of PFOB. Particle volume distributions for PFOB and oil emulsions were determined in triplicate (nominal mean particle diameter of approximately 210 nm and 200 nm, respectively) with a laser-light-scatter, submicron-particle-size analyzer (Zetasizer 4, Malvern Instruments Inc., Southborough, MA). The 10 and 90 percentile values for the particle size were 135 nm and 280 nm for the PFOB emulsion and 140 nm and 270 nm for the oil emulsion.

Agar Samples and Targeting

Agar gel was formed by boiling a 2% mixture of agar powder (Sigma-Aldrich) in distilled water. The molten agar was poured into a smooth, flat plastic tray and allowed to cool and gel into a flat sheet approximately 3 to 4 mm thick. A cork borer was used to core out circular pieces from these sheets, yielding cylindrical samples 18 mm in diameter. The samples were each placed individually in cell culture plates (12-well Costar® polystyrene microplates, Corning Incorporated, Corning, NY). Samples were then kept refrigerated (4°C) and immersed overnight in 3 mL of a solution of coating buffer (0.05 M carbonate-bicarbonate buffer, pH 9.6, Sigma-Aldrich) and avidin (250 μg per sample, ImmunoPure avidin, Pierce Biotechnology, Rockford, IL). Completion of this step yielded agar samples coated with avidin, to which biotinylated nanoparticles could be bound. The samples were gently rinsed with distilled water to eliminate unbound avidin, and then immersed in 3 mL of 100 mM phosphate buffer, to which 5 μL of biotinylated nanoparticle emulsion was added. After 2 hrs of incubation

with gentle agitation, the samples were gently rinsed to eliminate unbound nanoparticles, and placed in a room temperature (19°C) waterbath for acoustic microscopy.

Several different sample treatments were utilized for this portion of the study to examine scattering across a concentration range of high-contrast nanoparticles bound to substrate. Groups of agar blanks were exposed to mixtures of PFOB (high contrast) and oil (low contrast) emulsions in percentage ratios of 100:0, 80:20, 60:40, 40:60, 20:80, and 0:100 (n=3 for each group). An additional group of samples was left untreated to determine the baseline reflectivity amplitude for the agar surface.

Cell Samples and Targeting

Animal protocols were approved by the Animal Studies Committee at Washington University. Aortic smooth muscle cells (SMC's) were harvested from a one-year old female domestic pig immediately after sacrifice with Euthasol® (0.2 mL/kg, Virbac Corporation, Ft. Worth, TX). Approximately 15 cm of the abdominal aorta was excised, rinsed with saline, and sliced into 2-cm long sections. The adventitia was teased off to expose the medial layer, which was then gently scraped with dry sterile gauze to remove remaining adventitial cells. Each section was then cut longitudinally, and the intimal layer was removed by dry scraping with sterile gauze. The sections, now free of advential and intimal cells, were rinsed with saline and minced into 0.5 cm^2 pieces. Each piece was placed flat into a dry T75 tissue culture flask with the intimal side down. After sitting for 15 minutes, the flask surface was slowly flooded with smooth muscle cell culture growth medium (Clonetics SmGM-2, Cambrex Bio Science, East Rutherford, NJ). Cells were allowed to grow to confluence (approximately 3 wks), trypsinized, counted, and reseeded as per experimental design. This procedure yielded aortic SMC's that constitutively expressed tissue factor at the cell surface when cultured.

SMC samples for this study were prepared by plating cells on 12-mm diameter, microporous membrane culture plate inserts (Millicell HA with membranes composed of mixed cellulose esters, Millipore, Bedford, MA) and allowing the cells to grow to confluence (48 hrs). A subset of the samples was used to determine the number of cells growing on the substrate. The cells were detached with trypsin, resuspended and counted using a hemacytometer (Hausser Bright-Line, Horsham, PA), yielding counts between 70,000 and 100,000 cells/insert. For tissue factor targeting on the cell surface, a polyclonal antibody to the extracellular domain of recombinant porcine tissue factor was generated in rabbits (furnished by Dr. Eser Tolunay, Monsanto Company, St. Louis, MO) according to methods previously described (Lanza et al. 2000), and subsequently biotinylated according to standard methods for use as a targeting ligand.

Several sample groups were utilized for this portion of the study. The cells were maintained in smooth muscle growth medium (Clonetics SmGM-2) in a 37°C incubator throughout the targeting treatment. Nanoparticles were targeted to sites of tissue factor expression on the cells using a three-step avidin-biotin process, which entailed: 1) 60 min exposure to excess biotinylated anti-tissue factor antibody (125 μg per sample) under gentle agitation; 2) 60 min exposure to excess avidin (125 μg per sample); and 3) 60 min exposure to biotinylated PFOB nanoparticle emulsion (25 μL per sample). Samples were rinsed with serum-free smooth muscle growth medium between each step. Cell samples were targeted in this manner with either biotinylated PFOB nanoparticles (n=6), biotinylated oil-based nanoparticles (n=5), or a 1:1 mixture of biotinylated PFOB and oil nanoparticles (n=6). Another group (n=6) was treated in the same fashion but without initial administration of the biotinylated antibody, in order to assess the amount of non-specific binding. An additional group (n=5) of cell cultures was left untreated.

Ultrasound Data Acquisition and Analysis

Ultrasound data were acquired using a custom designed acoustic microscope (Figure 1). Samples were scanned in a waterbath using a 25 MHz immersion transducer (6-mm diameter, 25-mm focal length, model V324, Panametrics, Waltham, MA). The transducer was operated in pulse-echo mode using a broadband pulser-receiver unit (Panametrics 5900). A computer-controlled motorized gantry (Unidex 12, Aerotech, Inc., Pittsburgh, PA) was used to translate the transducer across the sample in a 35×35 or 40×40 point grid with 250-μm point spacing. Radiofrequency (RF) data was acquired at each point and digitized to 8 bits at a sampling rate of 500 MHz using a card-based digitizer (CS82G, Gage Applied Technologies, Lachine, Quebec, Canada). The data were stored as 2048-point waveforms for offline analysis.

Agar samples were scanned at room temperature, with the transducer positioned such that its focus was at the targeted surface. The acquisition window for the agar samples was timed to include only the reflection from the targeted surface. A single waveform acquired from the reflection from a flat steel plate was used as a reference. For the smooth muscle cell samples, the culture plate inserts were each completely filled with growth medium, then covered and sealed with acoustically transparent plastic film (Saran Wrap^{TM}) and placed in the water bath. The watherbath was maintained at 37°C, and the cell-covered upper membrane surface was positioned to be in the focal plane of the insonifying transducer. The reflected signals within the digitizer's acquisition window from each culture plate insert included the echoes from both the upper and lower surfaces of the cellulose substrate because of the relative thinness of the substrate. Thus, a rectangular gating window was applied to each sample waveform to isolate only the reflection from the upper (i.e., cell-covered) surface. Gate placement was determined automatically by a thresholding algorithm implemented in LabVIEW (National Instruments, Austin, TX).

For all samples, the spectral power was computed for the gated waveforms at each scan point, and subtracted in the log domain from the spectral power of the steel plate reflection waveform. The resulting transfer function was averaged over mid-band frequencies to yield integrated backscatter in dB for the corresponding scan point. This data was mapped to grayscale and used to create a C-scan image of the targeted surface for each sample. Mean integrated backscatter values for each sample were computed from the average across the entire surface.

Gas Chromatography

The samples from each treatment group were then processed for determination of the total amount of bound perfluorocarbon, through the use of gas chromatography with flame ionization detection and a bonded phase column (Model 6890, Agilent Technologies, Inc. Wilmington, DE). For each SMC sample, the intact cellulose membrane (with adherent SMC's) was cut out of the cell culture insert and processed, whereas each agar sample was utilized in its entirety. Each sample was combined with 20% KOH in methanol and homogenized. The resulting suspension was then combined with 2.0 mL of internal standard (0.1% octane in Freon), agitated continuously with a shaker for 30 minutes, and the lower extracted layer filtered through a silica gel column. Initial column temperature was 45°C and was increased to 145°C at a rate of 10°C/min.

RESULTS

Backscatter from PFC versus oil-based nanoparticles

Typical reflected RF data from agar surfaces left untreated or targeted with emulsions composed of only PFOB or oil-based nanoparticles are shown in Figure 2a. Note that the oil-based nanoparticles impart negligible surface reflectivity enhancement, in contrast to the surface targeted with PFOB nanoparticles, which exhibits substantially increased reflectivity

with respect to untreated agar. Example RF data from non-targeted SMC samples and SMC samples exposed to targeted PFOB or oil-based nanoparticles are shown in Figure 2b, as well as indications of typical time gate placement used to separate the echo from the cell-covered upper surface from the uninteresting back wall reflection. Again, note the greater signal amplitude of the RF data from surfaces enhanced with targeted PFOB particles.

Results of C-scanning across the surface layer of targeted agar are shown for specific examples from each treatment group in Figure 3a, with higher levels of backscatter depicted in lighter shades of gray. Relatively uniform backscatter is observed across the sample surface, and reflectivity increases with exposure to nanoparticle mixtures containing a greater proportion of PFOB nanoparticles. The low contrast oil-based particles create no observable enhancement in backscatter relative to the untreated samples (mean enhancement was less than 1 dB for either agar or cell samples). C-scans of the targeted smooth muscle cell cultures (Figure 3b) yielded similar results, although there was more variability in surface coverage of individual samples due to variations in the distribution of cells. Comparison of the backscatter averaged over the surface for each untreated and oil nanoparticle-targeted SMC sample using a student's t-test show no significant difference between the two groups ($p = 0.79$), confirming the lack of acoustic enhancement associated with the oil-based nanoparticles. These observations indicate that the component properties (e.g., speed of sound/compressibility) of the two types of nanoparticles are important determinants of the augmentation of backscatter, as demonstrated in previous studies (Marsh et al. 2002a). The oil vs. PFOB particle competition experiment illustrates the expected reduction of backscatter to the extent that receptor sites are occupied by low contrast oil-based nanoparticles.

Quantitative relationship between backscatter and nanoparticle binding

The quantitative relationship between backscatter and the absolute amount of PFOB bound to individual sample surfaces is depicted in Figure 4a (agar) and 4b (smooth muscle cells). The backscatter increases monotonically with bound PFOB for both sample types, with a decreasing rate of change at higher PFOB concentrations. The total amount of bound PFOB spans a larger range for the targeted cells relative to targeted agar, and reflects an increased amount of particle binding associated with the cells. Absolute levels of backscatter are also greater for the cell samples than for the agar samples, because of the substantially greater reflectivity of the underlying substrate (cellulose membrane). Although the use of targeting mixtures of approximately 50% oil and 50% PFOB particles might be expected to associate about half of the available receptors with nonreflective particles, the effect on backscatter is nearly saturated as indicated by the apparent asymptotic behavior in the graphs. This suggests that additional binding of high contrast PFC nanoparticles might yield only modest additional backscatter beyond some limiting value for the surface concentration of PFOB and/or nanoparticle occupancy of receptors, presuming equivalence of binding potential.

In order to quantify the statistical significance of the relationship between reflectivity augmentation and nanoparticle surface coverage, a simple asymptotic exponential model of the form $y = A\,(1 - e^{-Bx})$ with adjustable parameters A and B was fit to the reflectivity enhancement as a function of amount of bound PFOB. Reflectivity enhancement for a sample was defined to be the difference between the sample's backscatter and the mean value of the backscatter from all samples in the associated untreated group. Groups exposed to purely oil-based nanoparticles were excluded from the regression because there was no possibility of dependence of enhancement on the presence of PFOB for those groups. The enhancement data and corresponding model fits are shown in Figure 5 for (a) agar and (b) smooth muscle cell samples, with r^2 values of 0.88 and 0.89, respectively. Values of adjustable parameters were A=15.9±1.1 and B=0.035±0.008 for the agar samples, and A=9.35±0.89 and B=0.0032±0.0008 for the SMC samples. A high degree of confidence ($p<0.001$) was found for all parameter

estimates, indicating a highly significant (i.e. non-random) correlation between backscatter and bound PFOB exists that could be explained by the model.

DISCUSSION AND SUMMARY

These data illustrate the potential for targeted PFC nanoparticles to augment acoustic reflectivity from surfaces after binding to a selected epitope for two quite different molecular epitope geometries: flat, artificial surfaces versus irregular, living cell surfaces. The specificity of enhancement was confirmed by utilizing similar sized low contrast oil-based particles that did not affect reflectivity, and in competitive binding experiments with mixtures of low and high contrast particles that produced intermediate levels of contrast enhancement. Reflectivity enhancement was significant, asymptotically approaching 9 dB for smooth muscle cell monolayers on cellulose substrates and 16 dB for flat agar surfaces when targeting with PFOB nanoparticles alone.

Despite the differences in the substrate to which the particles bind, the binding profiles shown in Figure 5 were both described by curves of the form $y = A\,(1 - e^{-Bx})$ with similar levels of statistical significance. However, a relatively greater amount of PFOB was associated with the targeted cell samples as compared with targeted agar samples. The fact that the targeted nanoparticles accumulated in large amounts on the cells could be attributable to several factors. It is well known that smooth muscle cells grown to confluence in culture organize into heterogeneous “hill and valley” growth patterns, with regions that are densely populated with overlapping webs of cells, as well as regions that are only sparsely populated with cells (Chamley-Campbell et al. 1979;Powell et al. 1994). This nonuniform topography, along with the many irregular undulations, interstices, and fimbria that characterize individual living cells, may in fact have an exposed surface area that is quite large in relation to the planar substrate on which it is grown, thus yielding many more viable binding sites than might initially be assumed. A scanning electron micrograph is shown in Figure 6 of a typical culture of untreated SMC’s grown in the manner described above, to illustrate these characteristics. Based on these observations, the variation observed in the C-scans shown in Figure 3b is not surprising.

While the heterogeneity in surface topography associated with the SMC samples is readily apparent, the height variations are nonetheless likely to be smaller than a wavelength at 25 MHz (~60 μm). Many in vivo applications of molecular imaging will likely take place at lower frequencies (<10 MHz) and would presumably be less sensitive to these variations. Such applications may entail targeting of surfaces that range from being fairly smooth and regular (e.g. endothelium in larger vessels) to being much less planar and somewhat “rough” in an acoustic sense (e.g. fibrin networks in thrombi). Regardless, the measurements presented here, along with previous work demonstrating enhancement with plasma clots (Marsh et al. 2002a), illustrate that targeting efficacy with liquid perfluorocarbon nanoparticles clearly is achievable under a wide range of circumstances and for a wide range of substrates.

It was convenient to use a relatively high frequency for the in vitro studies described here in order to obtain sufficient temporal and spatial resolution to detect any heterogeneity in targeting or morphology of the samples. This frequency range is consistent with that used routinely in interventional arenas where the particles could be imaged with intravascular ultrasound (IVUS), as has been previously demonstrated in an animal model using 30-MHz IVUS (Lanza et al. 2000). Although theoretical models for the enhancement produced by nanoparticles bound to a surface (Marsh et al. 2002a;Couture et al. 2006) predict increased reflectivity at higher frequencies, substantial backscatter enhancement has also been observed from nanoparticles targeted to fibrin at 7.5 MHz in vitro and in an animal model (Lanza et al. 1996). The sensitivity of ultrasound to targeted nanoparticles for molecular imaging in a clinical setting may also be

enhanced through the use of novel signal processing schemes (Hughes et al. 2006) that detect changes in waveform shape not apparent with traditional energy-based measurements.

Previous results in vivo with inducible tissue factor in balloon injured carotid arteries illustrated contrast enhancement for distributed collections of bound particles (Lanza et al. 2000). The objective of the present work was to gain more comprehensive appreciation for the relationship between the concentration of bound high-contrast particles and the ultrasound signals emanating from targeted surfaces. The monotonic increase in signal as a function of particle concentration lends support to the notion that greater backscatter represents increased concentrations of particles regardless of geometric arrangements, vis-à-vis similarities in reflected waveform shape between two dissimilar substrate surfaces (Figures 2a and b). The presence of a potential asymptote for backscatter levels at higher particle concentrations could impose an upper limit on the ability of this system to quantify particle concentration, but would not affect the capacity for ultrasonic detection of sparse epitopes.

A transmission line model has been used in previous studies (Hall et al. 2001;Marsh et al. 2002a;Marsh et al. 2002b) to predict the magnitude and frequency dependence of reflectivity enhancement for nanoparticles targeted to a surface, with the simplifying assumption that the nanoparticles approximate a thin, uniform layer of liquid perfluorocarbon spread homogenously across the substrate. In those studies, the model was useful in predicting the relative differences in reflectivity afforded by similar distributions of targeted nanoparticles composed of perfluorocarbon liquids with different physical properties, but this model typically underestimated absolute levels of scattering augmentation. In the present study, a more sophisticated model would likely be necessary to accurately predict enhancement from surfaces having more than one type of bound particle, and, in the case of the cell samples, non-uniform topography. The ad hoc curve fits shown in Figure 5 suggest an asymptotic relationship between enhancement and levels of bound PFOB, but do not yield direct insight into the underlying mechanisms responsible for this behavior. Recently, Couture et al. described a study in which the reflectivity of varying concentrations of glass beads (~5.1 μm diameter) or perfluorohexane nanoparticles (~340 nm diameter) passively deposited on flat surfaces was measured at high frequencies (15–60 MHz) (Couture et al. 2006). These results were compared with predictions from a linear scattering model that accounted for transducer diffraction patterns, particle and substrate physical properties, and density of particle coverage. The experimental results are qualitatively similar to what has been described above: their measurements for both glass and perfluorohexane particles showed a large and approximately linear dependence of the reflection coefficient on surface coverage at relatively low particle densities, which then reached an apparent maximum level before leveling off (and eventually decreasing, in the case of the glass particles) at higher coverage densities. Although the scattering model did not predict the saturation effect observed in the actual measurements for high particle concentrations, it did provide a relatively accurate estimation of enhancement in the (linear) regime of low particle coverage density. Models of this type may provide an additional tool for predicting acoustic enhancement from particles targeted to relatively sparse epitopes, and could potentially be extended to the inverse problem of determining relative epitope density from measured acoustic augmentation.

The potential clinical implications for these data and previous reports relate to both diagnostic and therapeutic applications. The use of these particles for detection of abundant molecular epitopes such as fibrin in thrombi seems straightforward (Lanza et al. 1995a;Marsh et al. 2002a), but the present data indicate potential sensitivity to more sparse concentrations of cell surface markers such as tissue factor. Importantly, the data suggest that while large confluent expanses of bound nanoparticles provide significant contrast enhancement as for the cell surfaces, even partial coverings might be useful for augmenting contrast on targeted surfaces as seen in the agar experiments. Furthermore, the lack of appreciable background contrast

signal with the use of standard nanoparticle preparations, in association with rapid binding kinetics characterized both by high affinity and high avidity binding (due to multiple binding events per particle), could serve to enhance conspicuity and efficiency of diagnosis.

Acknowledgements

The authors would like to thank Ralph W. Fuhrhop and Elizabeth K. Lacy for their contributions in nanoparticle formulation. This work was supported by the National Institutes of Health (EB002168 and HL042950) and the NIH National Cancer Institute (CA119342).

References

Alkan-Onyuksel H, Demos SM, Lanza GM, et al. Development of inherently echogenic liposomes as an ultrasonic contrast agent. J Pharm Sci 1996;85:486–90. [PubMed: 8742939]

Chamley-Campbell J, Campbell GR, Ross R. The smooth muscle cell in culture. Physiol Rev 1979;59:1–61. [PubMed: 108688]

Couture O, Bevan PD, Cherin E, et al. A model for reflectivity enhancement due to surface bound submicrometer particles. Ultrasound Med Biol 2006;32:1247–55. [PubMed: 16875958]

Hall CS, Marsh JN, Scott MJ, et al. Temperature dependence of ultrasonic enhancement with a site-targeted contrast agent. Journal of the Acoustical Society of America 2001;110:1677–84. [PubMed: 11572376]

Hughes MS, Marsh JN, Zhang H, et al. Characterization of digital waveforms using thermodynamic analogs: detection of contrast-targeted tissue in vivo. IEEE Trans Ultrason Ferroelectr Freq Control 2006;53:1609–16. [PubMed: 16964911]

Klibanov AL, Hughes MS, Marsh JN, et al. Targeting of ultrasound contrast material - An in vitro feasibility study. Acta Radiol 1997;38:113–20.

Lanza GM, Abendschein DR, Hall CS, et al. In vivo molecular imaging of stretch-induced tissue factor in carotid arteries with ligand-targeted nanoparticles. J Am Soc Echocardiogr 2000;13:608–14. [PubMed: 10849515]

Lanza GM, Wallace KD, Abendschein D, et al. Specific Acoustic Enhancement Of Vascular Thrombi In-Vivo With A Novel Site Targeted Ultrasonic Contrast Agent. Circulation 1995a;92:1239.

Lanza GM, Wallace KD, Scott MJ, et al. A novel site-targeted ultrasonic contrast agent with broad biomedical application. Circulation 1996;94:3334–40. [PubMed: 8989148]

Lanza GM, Wallace KD, Scott MJ, et al. Initial Description And Validation Of A Novel Site Targeted Ultrasonic Contrast Agent. Circulation 1995b;92:1238.

Leong-Poi H, Christiansen J, Klibanov AL, Kaul S, Lindner JR. Noninvasive assessment of angiogenesis by ultrasound and microbubbles targeted to alpha(v)-integrins. Circulation 2003;107:455–60. [PubMed: 12551871]

Liang HD, Blomley MJ. The role of ultrasound in molecular imaging. Br J Radiol 2003;76(Spec No 2):S140–50. [PubMed: 15572336]

Lindner JR, Song J, Xu F, et al. Noninvasive ultrasound imaging of inflammation using microbubbles targeted to activated leukocytes. Circulation 2000;102:2745–50. [PubMed: 11094042]

Marsh JN, Crowder KC, Hughes MS, et al. In vitro acoustic molecular imaging of tissue factor expressed by smooth muscle cells with stable liquid perfluorocarbon nanoparticle contrast agents. IEEE Ultrason Symp 2004;2:1102–5.

Marsh JN, Hall CS, Scott MJ, et al. Improvements in the ultrasonic contrast of targeted perfluorocarbon nanoparticles using an acoustic transmission line model. IEEE Trans Ultrason Ferroelectr Freq Control 2002a;49:29–38. [PubMed: 11833889]

Marsh JN, Hall CS, Wickline SA, Lanza GM. Temperature dependence of acoustic impedance for specific fluorocarbon liquids. Journal of the Acoustical Society of America 2002b;112:2858–62. [PubMed: 12509007]

Moons AHM, Levi M, Peters RJG. Tissue factor and coronary artery disease. Cardiovascular Research 2002;53:313–25. [PubMed: 11827681]

Powell RJ, Cronenwett JL, Fillinger MF, Wagner RJ. Effect of endothelial cells and transforming growth factor-beta 1 on cultured vascular smooth muscle cell growth patterns. J Vasc Surg 1994;20:787–94. [PubMed: 7966814]

Schumann PA, Christiansen JP, Quigley RM, et al. Targeted-microbubble binding selectively to GPIIb IIIa receptors of platelet thrombi. Invest Radiol 2002;37:587–93. [PubMed: 12393970]

Villanueva FS, Jankowski RJ, Klibanov S, et al. Microbubbles targeted to intercellular adhesion molecule-1 bind to activated coronary artery endothelial cells. Circulation 1998;98:1–5. [PubMed: 9665051]

Wallace KD, Lanza GM, Scott MJ, et al. Intravascular Ultrasound Detection Of Thrombi After Enhancement With A Novel Site Targeted Acoustic Contrast Agent. Circulation 1995;92:2800. [PubMed: 7586244]

Winter PM, Neubauer AM, Caruthers SD, et al. Endothelial alpha(v)beta3 integrin-targeted fumagillin nanoparticles inhibit angiogenesis in atherosclerosis. Arterioscler Thromb Vasc Biol 2006;26:2103–9. [PubMed: 16825592]

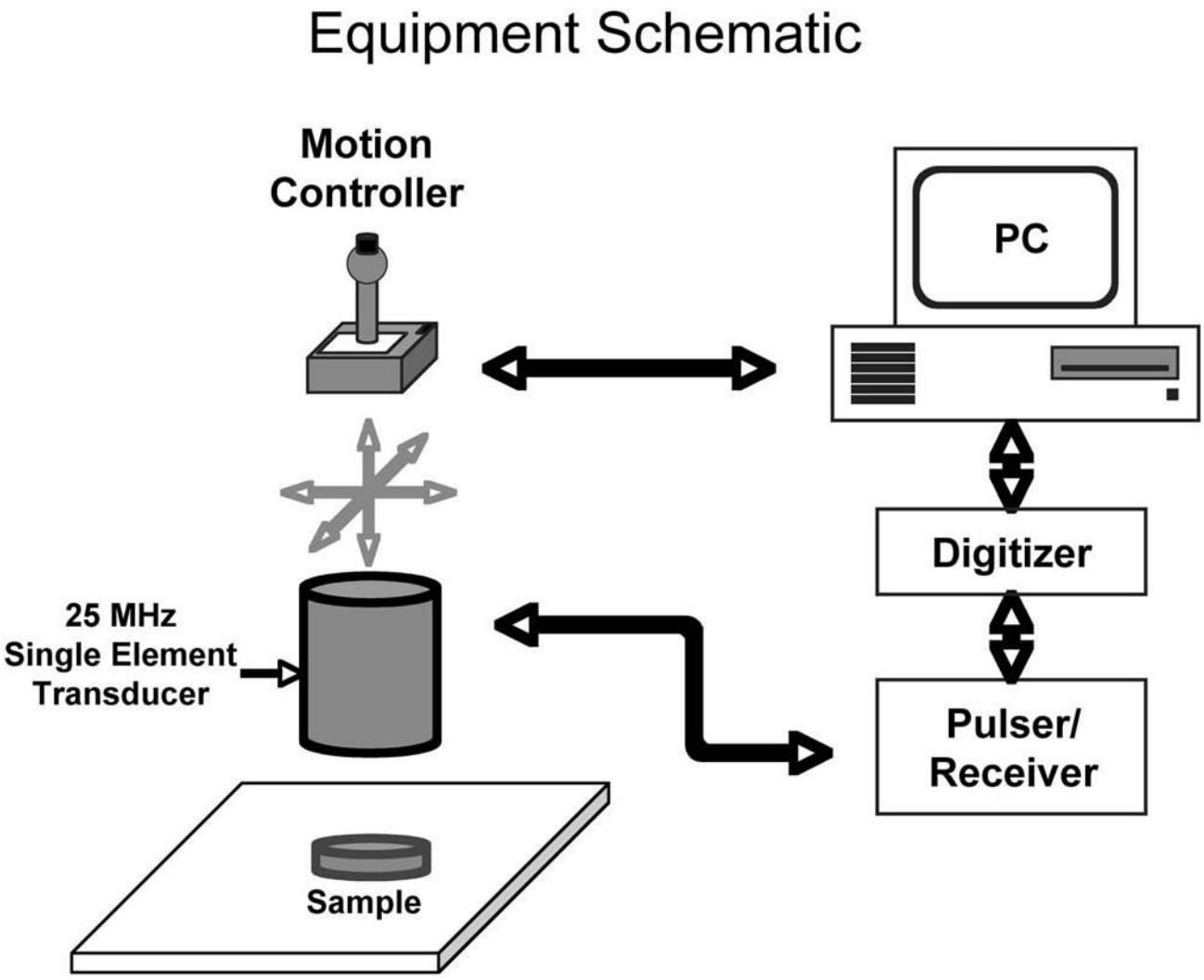

Figure 1.
Experimental setup. Samples were scanned in a waterbath at room temperature for agar samples, and at 37°C for cell cultures.

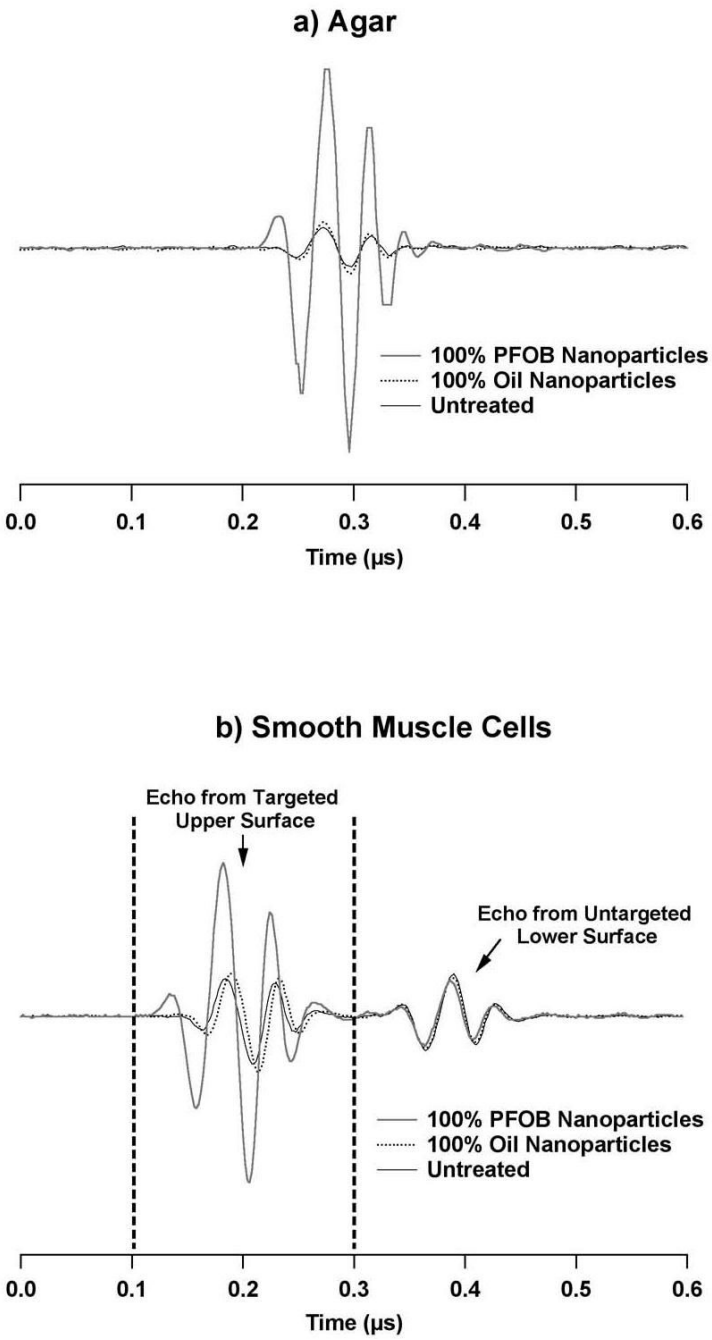

Figure 2.

Bottom: Example reflected RF data from surfaces of a) agar, and b) cultured smooth muscle cells grown on cellulose membranes. Waveforms are shown for untreated surfaces and surfaces targeted with high-scattering PFOB nanoparticles or low-scattering oil-based nanoparticles. In b), the time gate required for analysis is shown to illustrate the portion of the signal associated with the targeted, cell-covered upper surface of the cellulose substrate. The second echo is the reflection from the opposite surface of the cell culture substrate. Note in both a) and b) the greater RF magnitude from surfaces with bound PFOB nanoparticles.

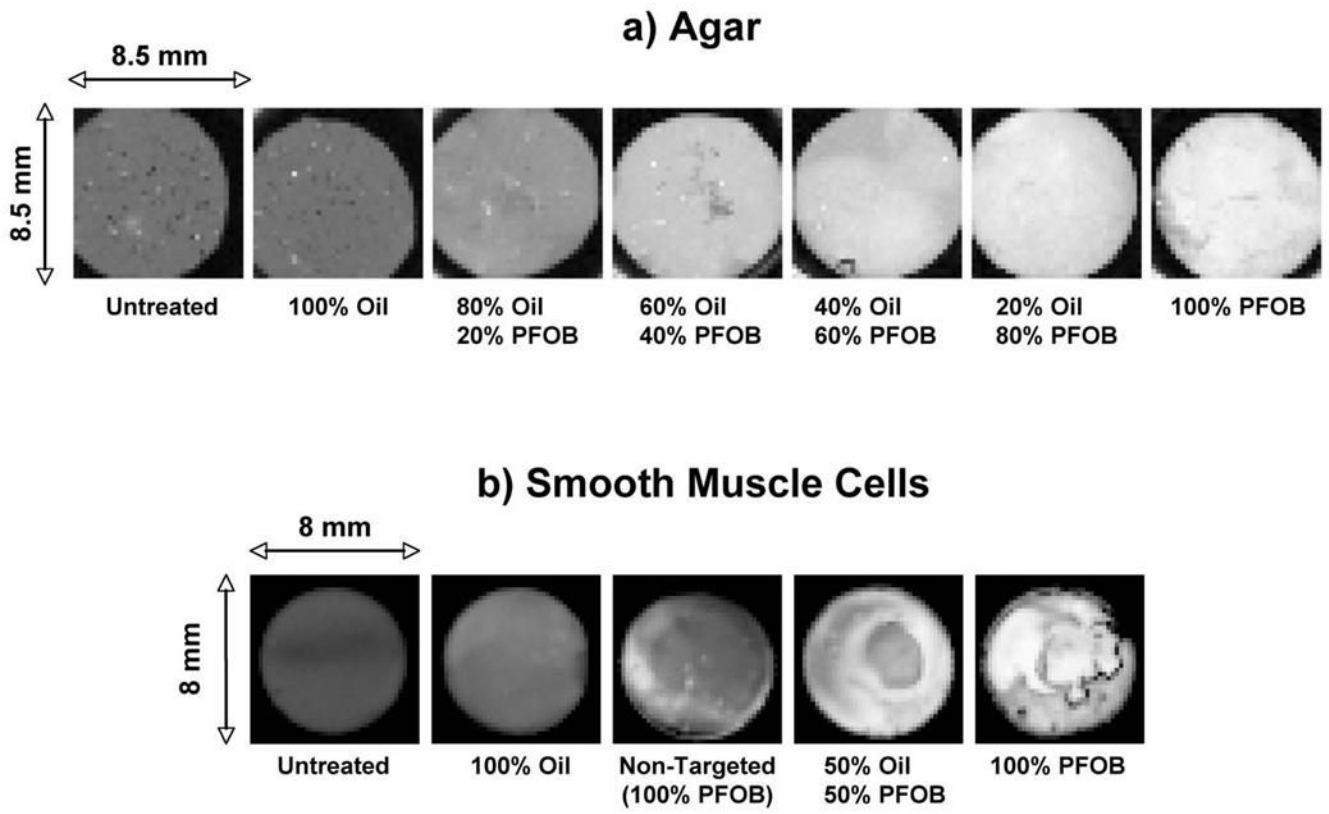

Figure 3.
"En face" example images of integrated backscatter from C-scanned sample surfaces under selected treatment conditions. a) Agar samples (white = −34 dB, black = −64 dB); b) Smooth muscle cell cultures (white = −10 dB, black = −28 dB).

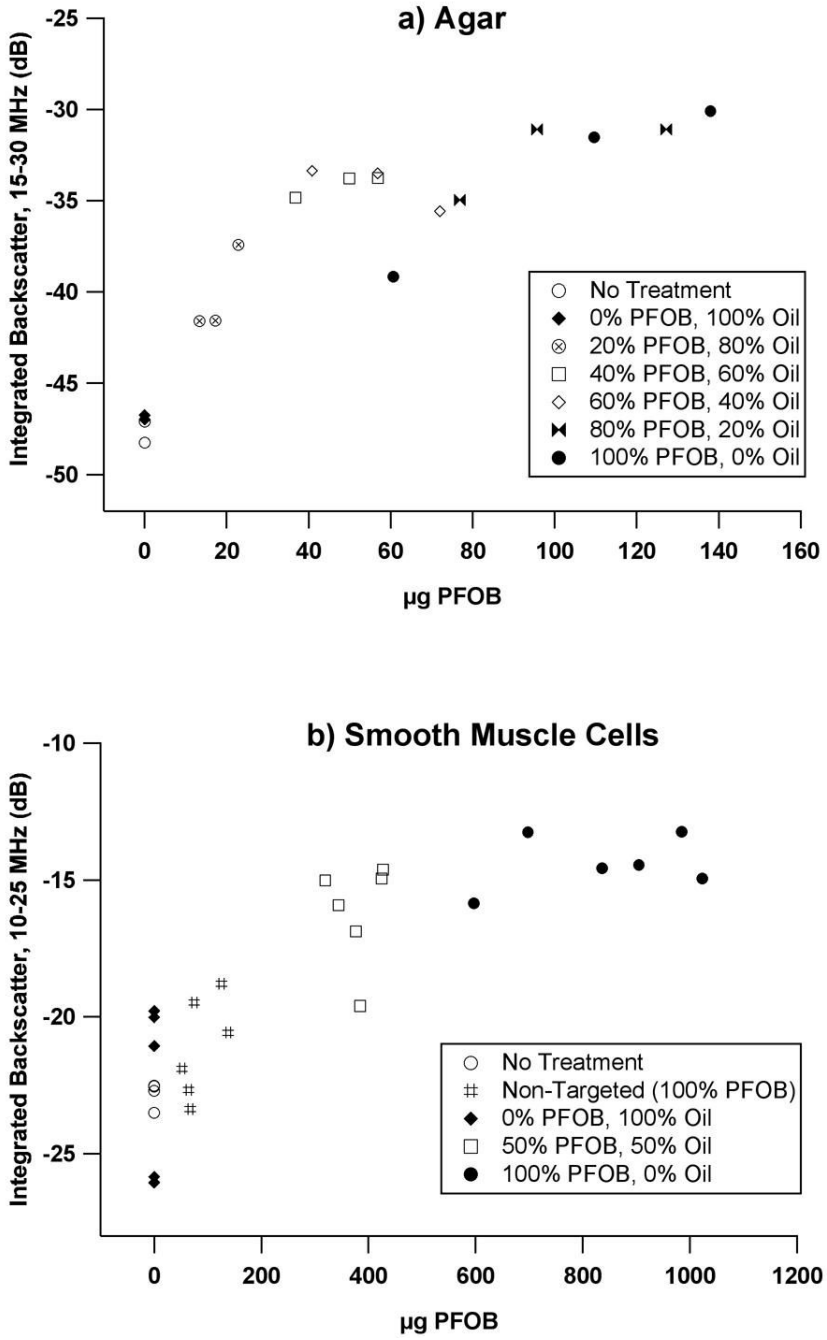

Figure 4.
Integrated backscatter vs. bound PFOB content for a) agar, and b) smooth muscle cells exposed to specific nanoparticle treatments.

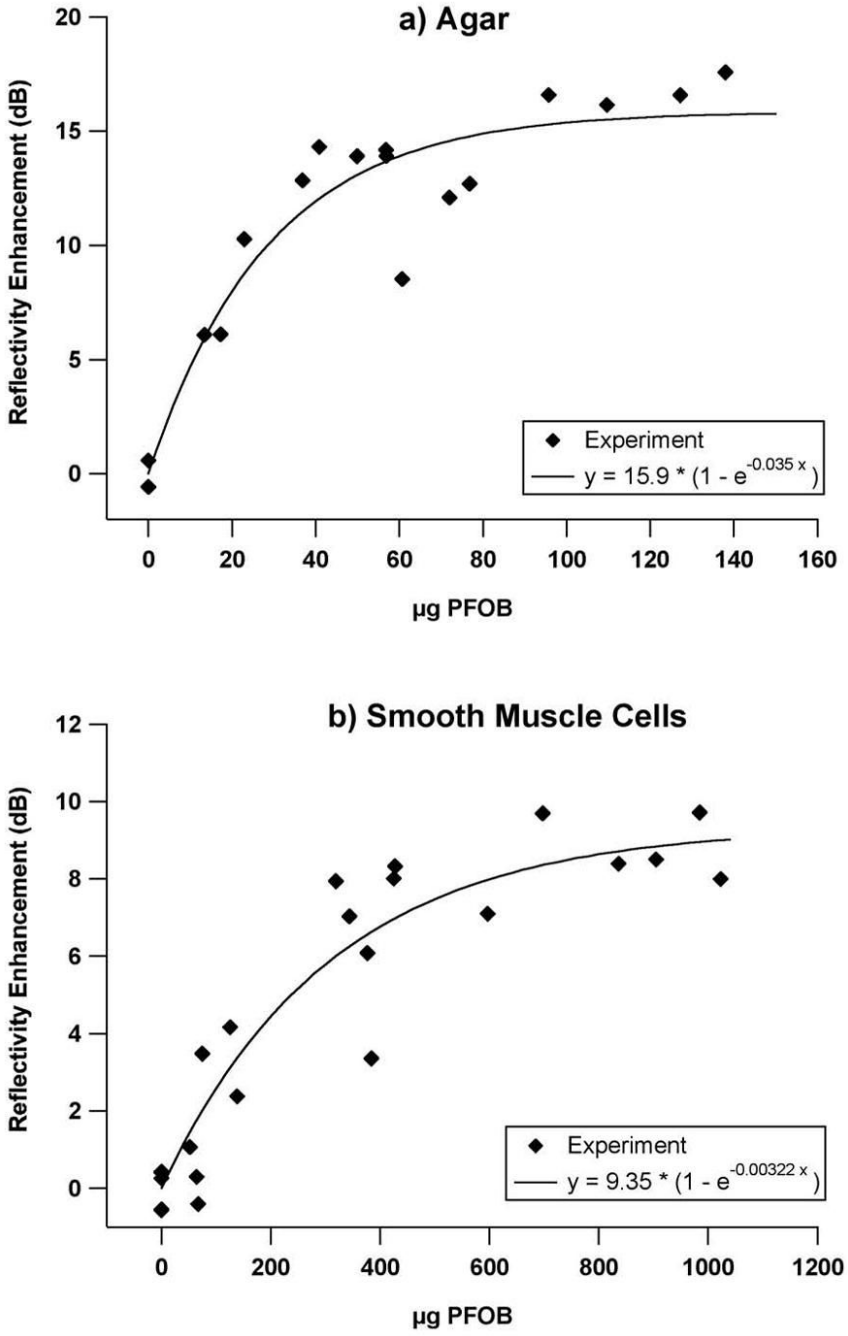

Figure 5.

Experimentally observed enhancement vs bound PFOB for a) agar, and b) smooth muscle cells exposed to PFOB nanoparticle mixtures (shown as data points), along with curve fits of the form $y = A(1 - e^{-Bx})$. Enhancement is defined as the difference in integrated backscatter of a treated sample from the mean value of untreated sample group. Values for adjustable parameters *A* and *B* are shown in the legend of each graph.

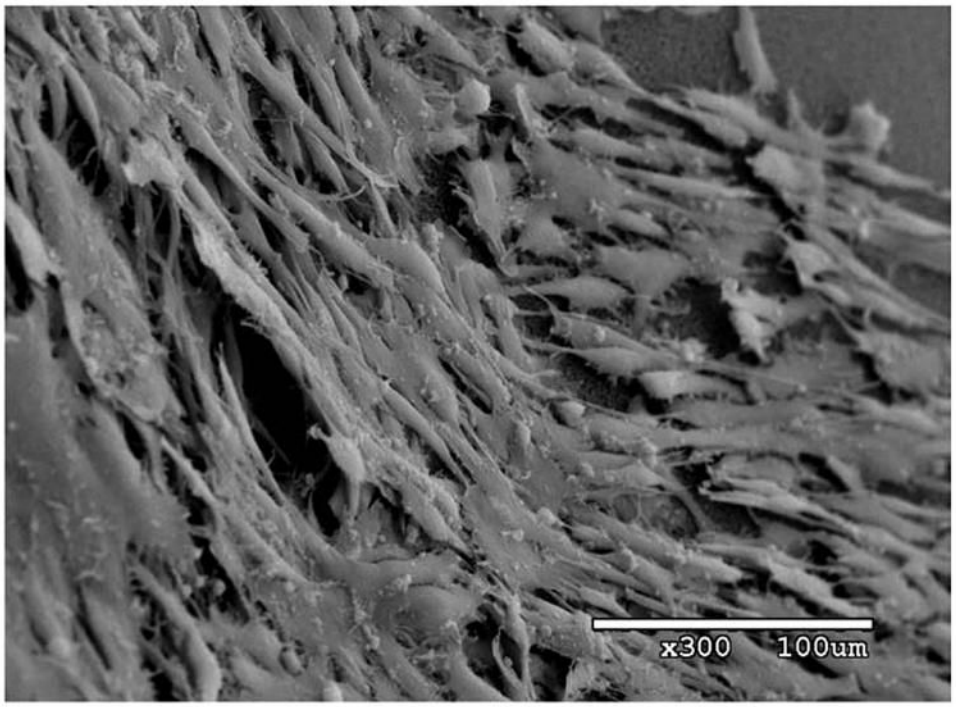

Figure 6.
Scanning electron micrograph of untreated porcine aortic smooth muscle cells grown in culture at 300X magnification. Heterogeneous and overlapping distribution of cells is clearly visible, as is irregular, dendritic shape of individual cells.